SPACE OBSERVATION OF PRE-MONSOON DROUGHT and HEAT WAVES

W. Timothy Liu and Xiaosu Xie

Jet Propulsion Laboratory, California Institute of Technology
Pasadena, C A 91109

w.t.liu@jpl.nasa.gov

KEY WORDS: monsoon, water cycle, rain, soil moisture

Abstract:

Space observations reveal that the drought and heat wave before summer monsoon onsets in India occur when more moisture advects out to Bay of Bengal (BB) than coming in from the Arabian Sea (AS). The vagary of summer monsoon onsets in India is described by the sharp increase in precipitation and soil moisture and sharp drop in air temperature. The monsoon season coincides with satellite observations of integrated moisture transport across the coast from the AS onto land and outflow to the BB; the influx of moisture agrees, in phase and magnitude, with precipitation on land. During the weeks before the monsoon onsets, India has the driest and hottest periods that often have adverse health and economic consequence. We show that the pre-monsoon drought and heat waves coincide with the net loss of moisture; moisture advected out to the Bay of Bengal before coming in from the Arabian Sea. The phase difference of moisture advection on the two sides of the subcontinent is caused by the earlier start of summer monsoon in the BB than in AS. The southwest wind of the summer monsoon starts at the peak of sea surface temperature rise which may cause atmospheric instability.

Introduction

"India heat wave kills 2,330 people as millions wait for rain," quoted from the CNN news headline on June 2, 2015. People have talked about the very hot and dry weather before the summer monsoon arrives in India. The heat and dryness may cause economic and agricultural disaster, besides human suffering. However, there is little scientific characterization of these pre-monsoon drought and heat waves.

Fig. 1 shows the longitude-time variations, averaged between 25°-26°N, across the middle of the India subcontinent; longitude from the AS to BB is represented on the horizontal axis and time runs up the vertical axis, from mid-April to Mid-June. Rainfall is from the Tropical Rainfall Measuring Mission (TRMM) on left, soil moisture from Aquarius in middle, and surface air temperature from Atmospheric Infrared Sounder (AIRS) on right. The summer monsoon starts in June, with sharp rises in rainfall and soil moisture, and sharp drop in air temperature. Just before the onsets, there are the hottest and driest weeks. These dry and hot periods, varies from one to a few weeks, are our pre-monsoon drought. Only two years 2012 and 2013 are shown as examples.

2 Spacebased Observations

Aquarius was launched in 2011 and failed in April 2015. The L-band sensors, such as those on Aquarius have a better penetration through vegetation. In this study, we make use of three years of soil moisture retrieved from Aquarius (Blindish et al. 2015). Soil moisture over the India subcontinent is computed from the Aquarius L3 data set at 1° resolution from August 25, 2011. The Aquarius data have approximately 7 day revisit time.

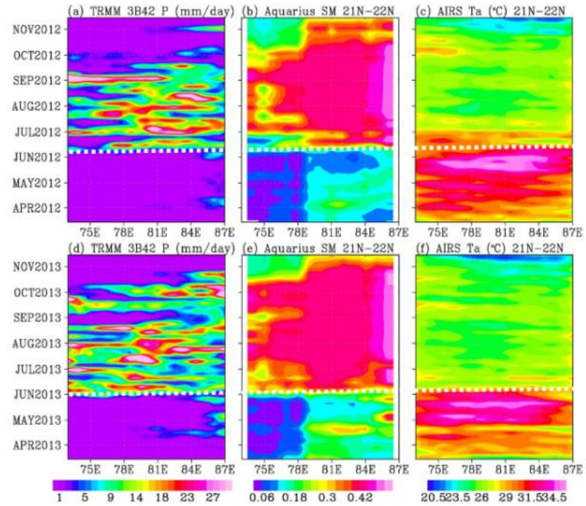

Fig. 1 Time-longitude cross sections of (a) precipitation, (b) soil moisture, and (c) surface air temperature, between 21°N-22°N. The data are from TRMM 3B42, Aquarius, and AIRS, and are 5-day average between April to October 2012. (d)-(f) are the same as (a)-(c), except for 2013.

Sea surface temperature (SST) data used in this study are from the TRMM Microwave Imager (TMI), at 0.25° grid for ascending and descending paths within 40° latitudes (Wentz et al. 2001) and produced by Remote Sensing Systems (RSS).

TRMM measures precipitation rate since December 1997, covering both ocean and land from 40°S to 40°N. TRMM 3B42 is a merged data set combining microwave and infrared precipitation estimates from 50°S to 50°N (Huffman et al. 2007). Rainfall over the India subcontinent is computed using the daily and 0.25° x 0.25° resolution data. TRMM mission was terminated in April 2015.

The surface air temperature is from version 6 of AIRS Level 3 standard gridded products with 1°x1° and daily resolution from the NASA Goddard Earth Sciences Data Information and Services Center. AIRS has provided temperature and humidity profiles in the atmosphere with accuracy comparable to those of conventional radiosondes since 2002 (Chahine et al. 2006).

In this study, 5-day averages of all the data are used.

3 INTEGRATED MOISTURE TRANSPORT

The computation of integrated moisture transport

$$\Theta = \int_0^{p_s} q\mathbf{u}dp$$

where p is the pressure, p_s is the pressure at the surface, q and **u** are the specific humidity and wind vector at a certain level, depends on the vertical profile of **u** and q, which are not measured from space directly. Statistical models were developed to related **Θ** to the equivalent neutral wind measured by scatterometers, cloud-drift winds at 850 mb, the integrated water vapor measured by microwave radiometers, based on Support Vector Regression. Xie et al. (2008) show the **Θ** derived from their statistical model agree with **Θ** derived from 90 rawinsonde stations from synoptic to seasonal time scales and from equatorial to polar oceans. Hilburn (2010) found very good agreement between this data set and data computed from Modern Era Retrospective-analysis for Research and Applications (MERRA) over the global ocean. Liu and

Xie (2014) shows that, for a total of 26,000 pairs randomly selected validation data, 2/3 from rawinsonde and 1/3 from the reanalysis, the root-mean-square (RMS) difference between the derived data and measurements is 57.5 kg/m/s and the correlation coefficient is 0.95 for zonal component, and 49.7 kg/m/s and 0.89 for meridional component, better than 10% of a range of approximately -600 to +600 kg/m/s. The data have been used to study the oceanic effect on terrestrial rainfall in South America (Liu et al. 2006) and Western Africa (Liu et al. 2012). In this study, surface wind vector from the European Advanced Scatterometer (ASCAT), available from 2007, and integrated water vapor from Special Sensor Microwave/Imager (SSM/I) are used to compute **Θ.**

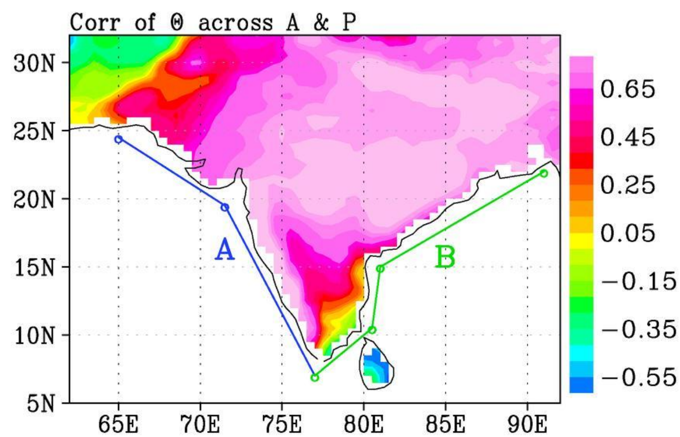

Fig. 2 Correlation coefficient between **Θ** across boundary A and precipitation. The monthly precipitation data are derived from TRMM 3B42 and **Θ** is derived from ASCAT and other data (Xie et al. 2008), from 3/2007 to 5/2015.

3 Relating Θ with monsoon

A good way to study monsoon onset is through **Θ.** Fig. 2 shows the strong correlation over most areas, between **Θ** integrated along the simplified coastline (A) and local rainfall over the subcontinent. **Θ** is projected normal to the coastline, positive directed from ocean to land and negative from land to ocean. Coastlines A is along the coast of AS and coastlines B is along BB. The time series for the years of 2012 and 2013 are shown in Fig. 3 as example. Starting between May and June, when **Θ** at the coast of AS (blue line) turns sharply positive, summer rainfall starts, but **Θ** at the coast of BB (green line) turns negative. The net transport (red line) is expanded in Fig. 3b and shown with the total rainfall over the land area. The difference between transport in and out of the continent (red line), largely falls out as rainfall. The rainfall and moisture influx agree approximately in magnitude and in phase. The direction of transport is reversed for the rest of the year. High soil moisture (cyan line) is also found in the periods of high rainfall. A slower variation in soil moisture than in rain can be discerned,

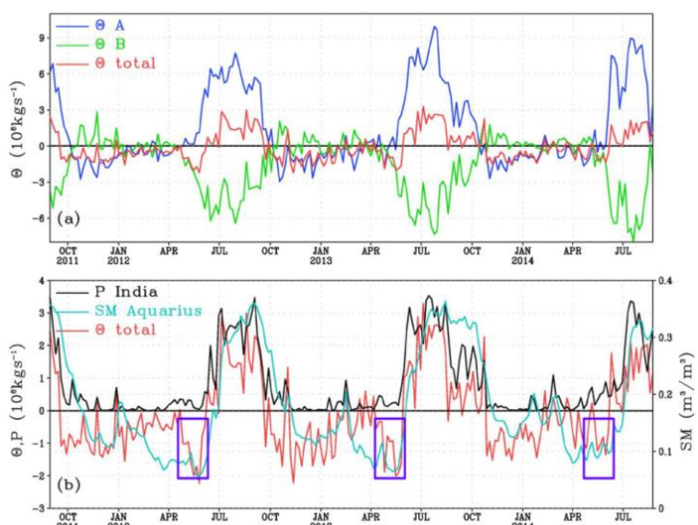

Fig. 3 (a) Time series of **Θ** across the western boundaries of India (A in Fig. 2, blue curve), **Θ** across the eastern boundaries (B in Fig. 2, green), and the sum (red). (b) Time series of precipitation (black) and soil moisture (light blue) averaged over the Indian subcontinent between 72°E-85°E and 10°N-30°N, and total **Θ** (red).

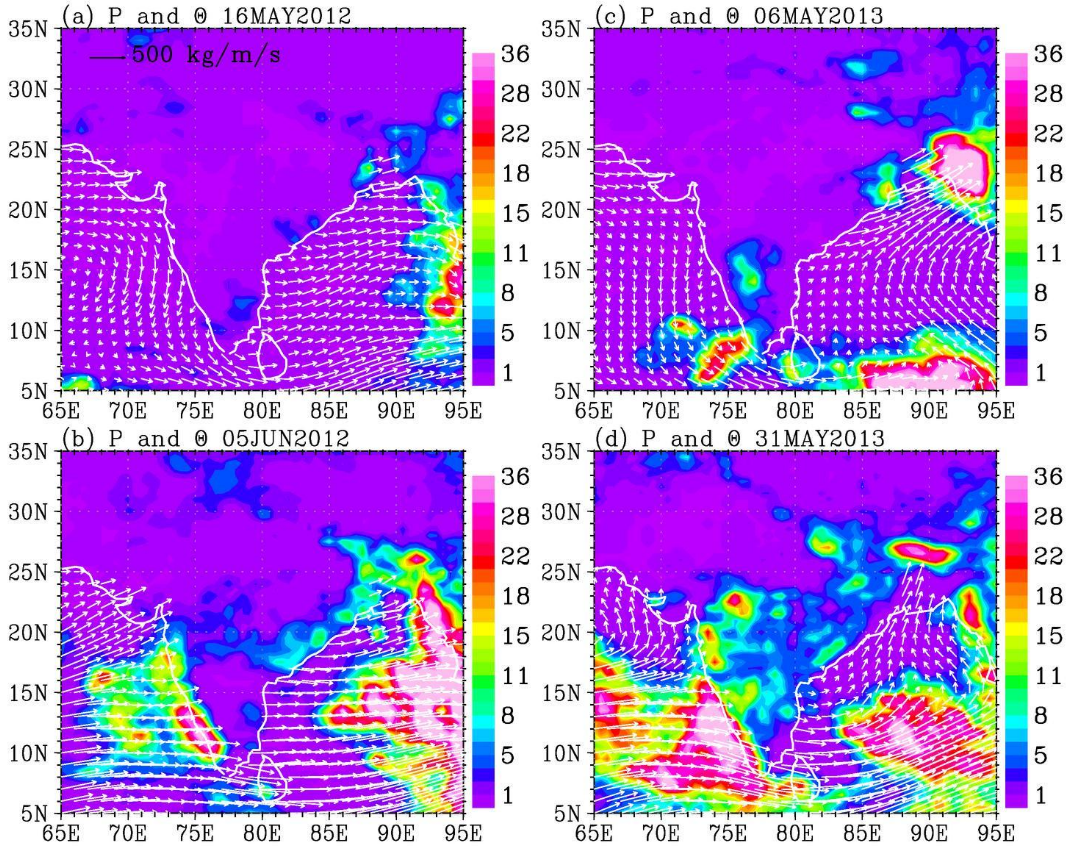

Fig. 4 Maps of precipitation rate (color) and **Θ** (white arrows) for 5 day averages during (a) May 16-20, 2012, (b) June 5-9, 2012, (c) May 6-10, 2013, and (d) May 31-June 4, 2013.

showing water retention by the soil. Soil moisture rises with rainfall, but does not drop as sharply as rainfall, in general.

4 Difference in Transport Across Two Coasts

Before the summer monsoon starts, early June in 2012 and late May in 2013, the net transport (red line) becomes negative; there is more moisture moving out to the BB than coming in from AS, with lowest soil moisture in the year (marked by boxes in Fig.3b). The negative moisture influx before monsoon onsets was first observed by Liu et al. (2005). During the pre-monsoon drought moisture is sucked out to the BB before it is replenished by those from AS. The difference is evident in the upper row of Fig. 4. On May 16, 2012, **Θ** from AS is weak, but **Θ** to BB is very strong. Similar difference is seen on May 6, 2013. Weeks later, on June 5, 2012 and May 31, 2013, summer monsoon was in full swing at the subcontinent, coming in from AS and out to BB (Fig. 4b and 4d). The surface winds from reanalysis of the European Centre for Medium-Range Weather Forecasts (ECMWF) in Fig. 5 show that the air sucked off to BB may draw hot and dry air from the northwest part of India.

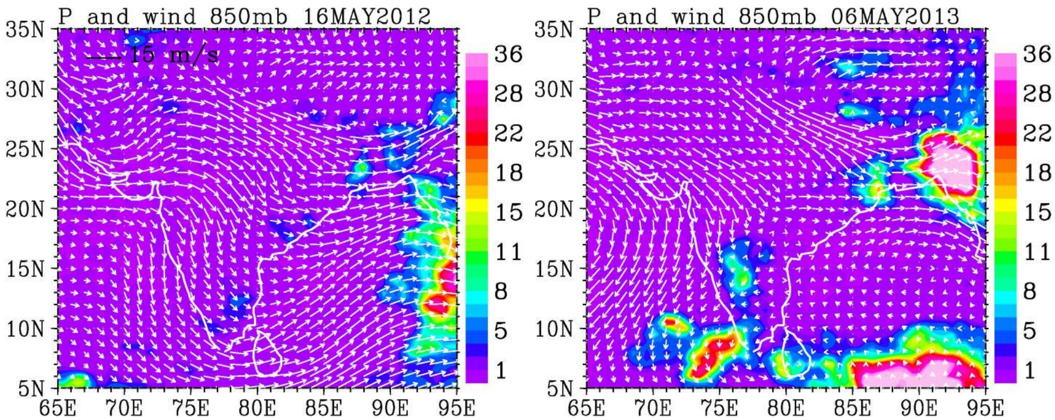

Fig. 5 Maps of precipitation rate (color) and 850 mb wind from ECMWF reanalysis (white arrows) for 5 day averages during (a) May 16-20, 2012, and (b) May 6-10, 2013.

5 Phase Difference of Monsoon Onsets Over Two Oceans

It is evident in Fig. 4 that the southeast summer monsoon starts earlier in BB than in AS, and is likely to be the cause of the pre-monsoon drought and heatwaves. There were many studies of summer monsoon onsets using collections of rain and wind measurement, and outgoing longwave radiation (e.g. Ahanthakrishnan and Soman 1988). Lau and Yang (1997), based on very limited rain data, showed that monsoon rainfall started in the South China Sea first then move to the Indo China and BB. They explained the progress of monsoon onset time through large-scale circulation from Tibetan Plateau and the Pacific warm pool. The lack of observation evidence was what started the South China Sea Monsoon Experiment.

If monsoon onsets in AS and BB are signaled by the rise of southwest winds (moisture transport), Fig. 6 will clarify the net loss of moisture from the Subcontinent. For the eight years between 2007 and 2014, the average zonal component of Θ in BB (green line) rises earlier than that in AS (blue line), by several weeks, resulting in a negative moisture transport into the subcontinent. For most of the years, SST peaks earlier in BB (black line) than AS (red line). Southwest wind or transport starts right after the peak of SST in both AS and BB. The exceptions are for the year 2009 and 2010, when SST in both oceans rose together, with small time lag between them, but there were still small negative moisture transport into the subcontinent in these two years. In 2011 and 2012, there were broad periods of warming in BB, without a sharp peak. In a few years, the monsoon onsets were disturbed by tropical cyclones. The rise of SST causes surface atmospheric instability and may be the regional cause of monsoon onset. This inference is consistent with the climatology analysis of Joseph et al. (2006) and Jiang and Li (2011).

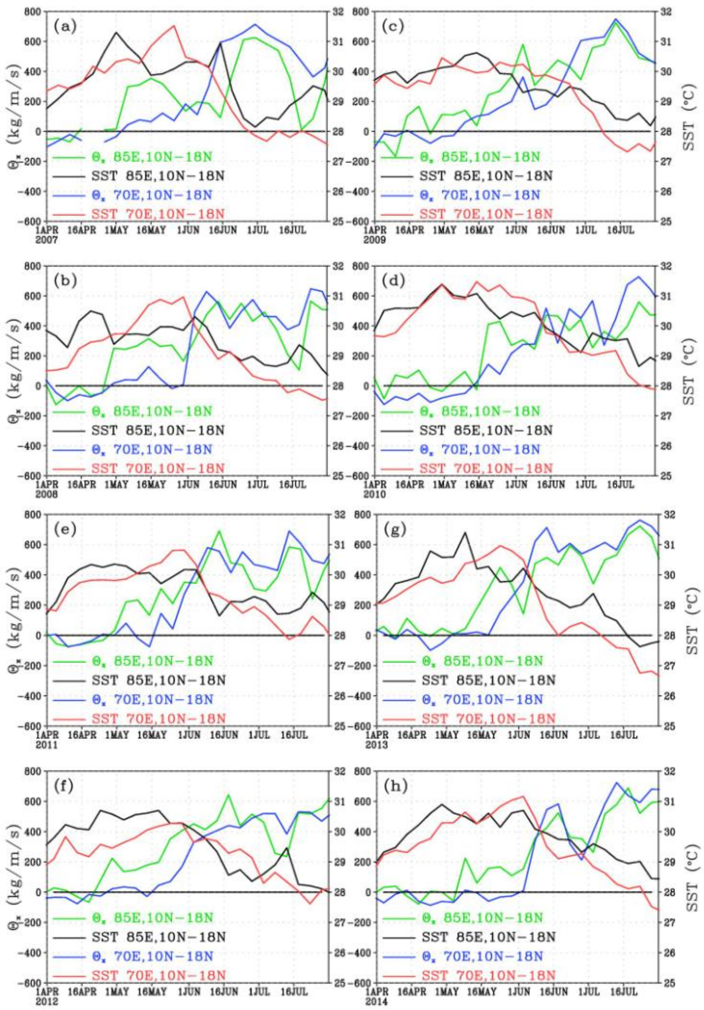

Fig. 6 Time series of SST (black) and **Θ** (green) over Bay of Bengal averaged along 85ºE and between 10ºN-18ºN, compared with SST (red) and **Θ** (blue) over Arabian Sea averaged along 70ºE and between 10ºN-18ºN.

Acknowledgment

This research was carried out at the Jet Propulsion Laboratory, California Institute of Technology, under a contract with the National Aeronautics and Space Administration (NASA). It was supported by NASA Precipitation Measuring Mission, NASA Energy and Water Cycle Studies, and Physical Oceanography Program of NASA
© 2015 California Institute of Technology. Government sponsorship acknowledged.

References

Ananthakrishnan, R. and M.K. Soman, 1988: The onset of the south-west monsoon over Kerala, 1901-1980. Int. J. Climatology, 8, 283-296.

Bindlish, R., et al. 2015: Global soil moisture from the Aquarius/SAC-D Satellite: Description and initial assessment. IEEE Geosci. Remote Sensing Letts 12(5): 923-927. doi: 10.1109/LGRS.2014.2364151.

Chahine, M. T., Pagano, S. Thomas, Aumann, H. Hartmut, R. Atlas, C. Barnet, J. Blaisdell, L. Chen, M. Divakarla, E.J. Fetzer, M. Goldberg, C. Gautier, S. Granger, S. Hannon, F. W. Irion, R. Kakar, E. Kalnay, B. H. Lambrigtsen, S.-Y. Lee, J. Le Marshall, W. W. McMillan, L. McMillin, E. T. Olsen, H. Revercomb, P. Rosenkranz, W. L. Smith, D. Staelin, L. L. Strow, J. Susskind, D. Tobin, W. Wolf, and L. Zhou, 2006: AIRS: Improving weather forecasting and providing new data on greenhouse gases, Bull. Amer. Meteor. Soc., 87, 911-926.

Hilburn, Kyle A., 2010: Intercomparison of water vapor transport datasets, presented at 17th Conference on Satellite Meteorology and Oceanography and 17th Conference on Air-Sea Interaction, Annapolis, MD.

Huffman, G.J., R.F. Adler, D.T. Bolvin, G. Gu, E.J. Nelkin, K.P. Bowman, Y. Hong, E.F. Stocker, D.B. Wolff, 2007: The TRMM Multi-satellite Precipitation Analysis: Quasi-Global, Multi-Year, Combined-Sensor Precipitation Estimates at Fine Scale. J. Hydrometeor., 8(1), 38-55.

Jiang, X. and J. Li, 2011: Influence of annual cycle of sea surface temperature on the monsoon onset. J. Geophys. Res. 116, D10105.doi:10.1029/2010JD015236.

Joseph, P. V., K. P. Sooraj, and C. K. Rajan, 2006: The summer monsoon onset over process over south Asia and an objective method for the date of monsoon onset over Kerala. Int. J. Climatol., 26, 1871–1893.

Lau, K.M. and S. Yang, 1997: Climatology and interannual variability of the Southeast Asian summer monsoon. Adv. Atmos. Sci., 14, 141-162.

Liu, W.T., X. Xie, and W. Tang, 2005: Monsoon, orography, and human influence on Asian rainfall. Proc. First International Symposium on Cloud-prone and Rainy Areas Remote Sensing. Hong Kong Chinese University Press. http://airsea.jpl.nasa.gov/publication/paper/CARRS-ms5.pdf

Liu, W. T., X. Xie, W. Tang, and V. Zlotnicki, 2006: Spacebased observations of oceanic influence on the annual variation of South American water balance. Geophys. Res. Lett., 33, L08710, doi:10.1029/2006GL025683.

Liu, W. T., X. Xie, and K. B. Katsaros, 2012: Observation of oceanic origin of Sahel precipitation from space, Remote Sensing of Environment, 123, 593-599.

Liu, W.T. and X. Xie, 2014: Ocean-atmosphere water flux and evaporation, Encyclopedia of Remote Sensing. E. Njoku (ed.), Springer-Verlag Berlin Heidelberg, 480-489. DOI: 10.1007/SpringerReference_327186.

Wentz, F. J., P. D. Ashcroft, and C. L. Gentemann, 2001: Post-Launch Calibration of the TRMM Microwave Imager, IEEE Transactions on Geoscience and Remote Sensing, 39(2), 415-422.

Xie X., W.T. Liu, and B. Tang, 2008: Spacebased estimation of moisture transport in marine atmosphere using support vector machine. Remote Sens. Environment, 112, 1846-1855.